REVISTA BOLIVIANA DE FÍSICA **38**, 15–26, 2021
ISSN 1562–3823. INDEXADA EN: SCIELO, LATINDEX, PERIÓDICA

EFFECTIVE HAMILTONIAN FOR A TIGHT-BINDING SQUARE LATTICE AND ITS RELATION TO A TWO-MESH LC CIRCUIT WITH DISCRETE CHARGE

HAMILTONIANO EFECTIVO DE UNA RED CUADRADA DE ENLACE FUERTE Y SU RELACIÓN CON UN CIRCUITO LC DE DOS MALLAS CON CARGA DISCRETA

EVARISTO MAMANI C. [1], MARCELO CALCINA-NOGALES [2], & DIEGO SANJINÉS CASTEDO [3] †
Instituto de Investigaciones Físicas, Universidad Mayor de San Andrés
Campus Universitario, c. 27 Cota-Cota, Casilla de Correos 8635
La Paz - Bolivia
(*Recibido 2 de septiembre de 2021; aceptado 18 de noviembre de 2021*)
https://doi.org/10.53287/qqjb7795ot66r

RESUMEN

En este trabajo consideramos una función hamiltoniana de enlace fuerte extendida a primeros y segundos vecinos para una partícula cargada que se transporta por saltos (*hopping*) en una red cuadrada en presencia de un campo estático arbitrario y un campo uniforme rápidamente oscilante con frecuencia ω. La aplicación del método semiclásico y el método de Kapitza de promediación temporal hasta $O(\omega^{-2})$ conduce a una función hamiltoniana efectiva (independiente del tiempo) con elementos de salto que dependen de los parámetros de los campos externos. Controlando dichos parámetros podemos manipular las interacciones de tal forma de emular un sistema físico diferente, en este caso, un circuito LC de dos mallas con carga discreta.

Descriptores: Método de enlace fuerte — modelo semiclásico — sistemas mesoscópicos.

Código(s) PACS: 31.15.aq, 03.65.Sq , 73.23.-b

ABSTRACT

We consider an extended tight-binding Hamiltonian function comprising nearest and next-to-nearest neighbor interactions for a charged particle hopping in a square lattice in the presence of a static arbitrary field and a rapidly oscillating uniform field with frequency ω. The application of the semiclassical method and the Kapitza's method for time-averaging up to $O(\omega^{-2})$ yields an effective (time independent) Hamiltonian function with long range hopping elements that depend on the parameters of the external fields. By controlling these parameters we can engineer the interactions in such a way as to emulate a different physical system, namely, a two-mesh LC circuit with discrete charge.

Subject headings: Tight-binding method — semiclassical model — mesoscopic systems.

1. INTRODUCTION

The study of effective Hamiltonians in solid state physics, derived with time-averaging procedures (originally due to P. L. Kapitza for the study of the inverted pendulum Kapitza (1965); Landau (1985) applied to tight-binding lattices, has recently acquired interest given the feasibility of managing (engineering) the hopping elements when the lattice is subject to external and rapidly oscillating driving fields. Some of the effects relevant for transport phenomena include, for example: dynamic localization, coherent control of tunneling, metal-insulator transitions, atomic motion in atom traps, effective next-to-nearest neighbor interactions and effective Bloch oscillation (Dunlap 1986; Rahav 2003; Bandyopadhyay 2008; Itin 2014, 2015; Mamani 2017). The idea of using an *extended* tight-binding Hamiltonian with a kinetic energy of the form $2\sum_n A_n \cos(nak)$ can be traced back to the work of Dunlap and Kenkre, (Dunlap 1986) where their results concerning dynamic localization are extended to long-range interactions in a 1D lattice with hopping elements A_n and lattice constant a. The case where all the interactions are considered led to the new concept of *exact* dynamic localization in the presence of an AC electric field (Dignam 2002). Such a concept of "band engineering" with long-range interactions has been also investigated (theoretically and experimentally[1] in optical lattices; Longhi

[1]https://orcid.org/0000-0002-3484-8582
[2]https://orcid.org/0000-0002-7926-8215
[3]https://orcid.org/0000-0001-6832-9513
†diegosanjinescastedo@gmail.com

[1] Many of the current theoretical models do not take into account some real physical effects (for simplicity), such as interband transitions, dispersion of the hopping particle by thermal collisions and phononic interactions, loss of crystal periodicity, etc., due which the particle's wavepacket usually decoheres rapidly and the observation

(2010); Madison et al. (1998) reported the first observation of dynamical suppression of the band due to an external AC field in an optical lattice whereby the bandwidth shrinks to zero and the Bloch states become localized when the field amplitude meets a condition that was also derived in Mamani *et al.* (Mamani 2017) using the semiclassical method.[2] More recent investigations in layered graphene systems show that the effects derived from an extended tight-binding Hamiltonian can be considered as improvements to the usual nearest neighbor model results (Reich 2002; Kundu 2011; Wright 2009; Kadirko 2013).

In this work we use an extended tight-binding Hamiltonian where the long-range interactions correspond to a *bidimensional* system, namely, an square lattice; then, we set about establishing a formal equivalence between that lattice and a two-mesh LC circuit with discrete charge by means of deriving and comparing their corresponding effective Hamiltonians (the case of a 1D lattice and its relation to the single-mesh LC circuit with discrete charge has been already studied by Mamani *et al.* (Mamani 2018). We show that such an equivalence is possible by managing the parameters of the driving oscillating field (with frequency ω) acting upon the square lattice such that the nearest neighbor interactions become effectively suppressed leaving the remanent next-to-nearest neighbor (2nd neighbor) interactions as the dominant ones at order ω^0 plus the 3rd neighbor interactions at order ω^{-2}. The theoretical framework for the study of quantum circuits with discrete charge is referred to Chen and Li (1996) wherein the fundamental commutator $[\widehat{q},\widehat{\phi}] = i\hbar$ is defined: nq_e are the discrete eigenvalues of the electric charge operator $\widehat{q}$ (n is an integer and q_e is the elementary electronic charge), the flux operator $\widehat{\phi} = -i\hbar\partial/\partial q$ is the conjugate of $\widehat{q}$ and the substitution $\widehat{\phi} \to (2\hbar/q_e)\,\mathrm{sen}(q_e\widehat{\phi}/2\hbar)$ takes into account the discrete nature of the electric charge (Flores 2005; Calcina-Nogales 2013; Flores 2002). The physical phenomena associated to these kind of systems have been reported: persistent currents, Bloch oscillations in quantum circuits, Coulomb blockade, current magnification, voltage and current engineering (Chen and Li 1996; Flores 2005, 2002; Chen 2005; Calcina-Nogales 2020), etc. These cases demonstrate the feasibility of modeling the physics of mesoscopic devices within the conceptual framework referred to above.

Although the one-dimensional and the square tight-binding lattices do not exist as such (to our knowledge), it seems that the reported discrete-charge mesoscopic systems would be soon technicaly feasible, thus, permitting the posibility of testing the predictions deduced from comparing both systems. In this sense, the semiclassical method together with the time-averaging techniques provide an easier and more straightforward way of deriving an effective Hamiltonian, as we could in fact verify in the derivation of the quantum effective Hamiltonian of the two-mesh LC circuit (Calcina-Nogales 2020). Besides, the semiclassical method also provides a bifurcation condition already studied in the one-dimensional lattice (Mamani 2018) and suggested in the two-dimensional case (in this work) that could be useful for predicting the transition between different electronic dynamical regimes.

The organization of our work is the following: in Section 2 we derive the effective Hamiltonian for a square lattice using the time-averaging technique and extending the procedures we have already used for the one-dimensional lattice (Mamani 2017); in Section 3 we apply the results of the previous section to the managing of the effective Hamiltonian hopping elements so as to emulate case of the two-mesh LC circuit with discrete charge; finally, in Section 4 we present the most important concluding remarks and point out some directions for future research.

2. DERIVATION OF THE EFFECTIVE HAMILTONIAN FOR THE SQUARE LATTICE

Consider the extended tight-binding Hamiltonian function with nearest-neighbor and next-to-nearest neighbor interactions for an independent test particle with charge q_e (i.e., we do not consider any possible interaction with like particles whatsoever neither the particle affects the distribution of the external electric fields acting upon it) which hops in a square lattice with cells of side a under the action of external electric fields,

$$H\,(x,y,k_x,k_y;t) = -2A\cos(ak_x) - 2B\cos(ak_y) \\ -2C\cos(ak_x)\cos(ak_y) + q_e\mathbf{r}\cdot\mathbf{f}(\omega t) + V(\mathbf{r}). \quad (1)$$

The tight-binding band in the Hamiltonian (1) has the standard form $-\sum_{m,n}\gamma_{m,n}\cos(\mathbf{k}\cdot\mathbf{R}_{m,n})$ where $\mathbf{k} = (k_x,k_y)$ and $\mathbf{R}_{m,n} = a(m,n)$; the hopping elements are $A = \gamma_{0,\pm1} = \gamma_{\pm1,0}$ for the nearest neighbors and $C = \gamma_{\pm1,\pm1} = \gamma_{\pm1,\mp1}$ for the next-to-nearest neighbors. In the following derivation, and in order to deal with a more compact notation, we take unitary numerical values for the lattice constant a and for the physical constants q_e, $\hbar$. $V(\mathbf{r})$ is an external arbitrary static potencial energy at $\mathbf{r} = (x,y)$ and $\mathbf{f}(\omega t) = (f_x,f_y)$ is the rapidly oscillating external driving field with frequency $\omega \gg 1/T$, where T is the particle's characteristic period of oscillation in the absence of the driving field. Without loss of generality and for the sake of simplicity, we will suppose that the external electric field $\mathbf{f}(\omega t)$ is an even function of t.

Although the quantum Hamiltonian corresponding to (1) with $V(\mathbf{r}) = 0$ has the spatial divergent potential $\mathbf{r}\cdot\mathbf{f}(\omega t)$, the problem of finding its eigenfunctions has been already widely treated in terms of the vector potential representation (Houston 1940; Krieger 1986; Kittel 1987; Rossi 1997) whereby the electric field is $\mathbf{f}(\omega t) = \partial\mathbf{g}/\partial t$, such that the momentum operator is shifted as $\mathbf{p} \to \mathbf{p}+\mathbf{g}$ within the kinetic energy operator. As a conse-

–for example– of Bloch oscillations is restricted to a few complete periods (c.f.: Lyssenko et al. (1997); Madison et al. (1998)). In the absence of such effects, the wavepacket's width may oscillate and eventually be restored to its initial value, as shown, e. g., by Dignam and de Sterke in the exact dynamic localization effect (Dignam 2002).

[2] A concise and pedagogical justification of the semiclassical method for a general periodic potential can be found, for example, in Ch. 12 of Ashcroft and Mermin (1976)

quence, the "acceleration theorem" $\partial\mathbf{k}/\partial t = \mathbf{f}(\omega t)$ is derived strictly quantum-mechanically in agreement with the semiclassical approach considered in our work.[3] For the case of $V(\mathbf{r}) \neq 0$ in (1), the gauge substitution $\mathbf{g} \to \mathbf{g} + \nabla V(\mathbf{r})t$ is made and the resulting acceleration theorem becomes $\partial\mathbf{k}/\partial t = \mathbf{f}(\omega t) - \nabla V(\mathbf{r})$.

We use now the Hamilton's equations which yield the time derivatives of the position and the momentum:

$$\dot{x} = H_{k_x} = 2A \operatorname{sen} k_x + 2C \operatorname{sen} k_x \cos k_y, \tag{2}$$

$$\dot{y} = H_{k_y} = 2B \operatorname{sen} k_y + 2C \operatorname{sen} k_y \cos k_x, \tag{3}$$

$$-\dot{k}_x = H_x = f_x(\omega t) + V_x, \tag{4}$$

$$-\dot{k}_y = H_y = f_y(\omega t) + V_y; \tag{5}$$

we set the notation $V_x, V_y, V_{xx}, V_{yy}, V_{xy} = V_{yx}$ and $H_{k_x}, H_{k_y}, H_x, H_y$ for the derivatives of $V(\mathbf{r})$ and $H(\mathbf{r}, \mathbf{k}; t)$ respectively; this notation will apply only to the Hamiltonian and potential energy functions hereafter. It will be convenient also to use the generic symbol z for either of the coordinates x, y where a simplified expression could be written. Let us now apply the canonical transformations between the momenta: $(z, k_z) \to (z, k'_z)$ given by $k'_z \equiv k_z + g_z$, whereby the "displaced momentum" k'_z is defined along with the time integral of the external field, $g_z \equiv \int^t f_z(\omega t')dt'$; this is the realization of the vector potential representation that yielded $\mathbf{k} \to \mathbf{k} + \mathbf{g}$ as projected onto the square lattice and which was already referred to. The substitution of these transformations in (2)-(5) yields:

$$\dot{x} = 2A \operatorname{sen}(k'_x - g_x) + 2C \operatorname{sen}(k'_x - g_x) \cos\left(k'_y - g_y\right), \tag{6}$$

$$\dot{y} = 2B \operatorname{sen}\left(k'_y - g_y\right) + 2C \cos(k'_x - g_x) \operatorname{sen}\left(k'_y - g_y\right), \tag{7}$$

$$\dot{k}'_x = -V_x, \tag{8}$$

$$\dot{k}'_y = -V_y. \tag{9}$$

Due to the action of the combined static and oscillating fields, $-\nabla V(x, y)$ and $\mathbf{f}(\omega t)$, the particle will move with small oscillations around a slow varying trajectory. Thus, we introduce the "slow" $Z(t)$, $K_z(t)$ coordinates and the "fast" $\xi_z(\tau)$, $\eta_z(\tau)$ coordinates in the direct and reciprocal spaces respectively; the fast coordinates are considered perturbations of the slow coordinates:

$$z(t) = Z(t) + \xi_z(\tau), \quad k'_z(t) = K_z(t) + \eta_z(\tau), \tag{10}$$

where $\tau \equiv \omega t$ is such that the time-average of $\xi_z(\tau)$, $\eta_z(\tau)$, vanish in the time interval with period $T = 2\pi/\omega$ while $Z(t)$, $K_z(t)$, remain almost constant in the same interval, i.e., $\langle \xi_z \rangle = \langle \eta_z \rangle = 0$, and $\langle Z \rangle = Z(t)$, $\langle K_z \rangle = K_z(t)$. We have used the definition of the time-average as $\langle \cdot \rangle = (1/T) \int_0^T (\cdot) dt$.

[3] In this sense, the semiclassical method provides *exact* results that coincide with the quantum ones, as we could verify in the above mentioned references and also in Dignam and de Sterke,(Dignam 2002) wherein a study of *exact* dynamical localization is carried on (we have work in progress in this direction).

The set of transformations

$$(x, y, k_x, k_y) \to (x, y, k'_x, k'_y) \to (X, Y, K_x, K_y) \tag{11}$$

is canonical since the structure of Hamilton's equations is preserved (Landau 1985):

$$\begin{aligned} \dot{z} &= H_{k'_z}(x, y, k'_x, k'_y; t), \quad \dot{k}'_z = -H_z(x, y, k'_x, k'_y; t), \\ \dot{Z} &= H_{K_z}(X, Y, K_x, K_y), \quad \dot{K}_z = -H_Z(X, Y, K_x, K_y); \end{aligned} \tag{12}$$

this is so as a consequence of the invariance of the Poisson brackets: $[k_z, z] = [k'_z, z] = [K_z, Z] = 1$ which yields $H(x, y, k'_x, k'_y; t) = H(x, y, k_x, k_y; t) + \partial F(x, y, k'_x, k'_y; t)/\partial t$ for some generating function $F(x, y, k'_x, k'_y; t)$ that can be readily calculated, and the time-averaging which gets us from $H(x, y, k'_x, k'_y; t)$ to $H(X, Y, K_x, K_y)$. The resulting shift of the time dependence from the $\mathbf{r} \cdot \mathbf{f}(\tau)$ term in $H(x, y, k_x, k_y; t)$ into the arguments of the kinetic energy operators in $H(x, y, k'_x, k'_y; t)$ is not only a convenient transformation (in order to get time-averages efficiently) but it is also a necessary one to render $\mathbf{k} = (k_x, k_y)$ as a "good quantum number" (Kittel 1987). Now, $H(X, Y, K_x, K_y) \equiv H^{eff}$ is the form of the effective Hamiltonian that, as a result of the Hamilton's equations, represents a constant of motion and whose explicit construction will be possible giving the resulting Eq.(18) at the end of this section. In this work we will restrict the potential energy to the quadratic form of the position coordinates $V(x, y) = c_1 x^2 + c_2 y^2 + c_3 xy$ since it is this kind of function that yields the correct physical interpretation for H^{eff} as a tight-binding Hamiltonian (the physical realization of such $V(x, y)$ onto the square lattice plane would be achieved –in principle– by placing the plane inside a dielectric cylinder shell with an specific surface charge distribution); otherwise, if $V(x, y)$ had the form of a higher degree polynomial function, H^{eff} could still be a valid Hamiltonian but not with the form of a tight-binding one (Mamani 2017).

By replacing the time-derivatives of the terms in (12) into the system (6)-(9) we obtain the system (B1)-(B4) in Appendix B wherein we applied the time-average techniques that yield the system for the effective dynamical coordinates:

$$
\begin{aligned}
(1/2)\dot{X} &= \widetilde{A}\,\mathrm{sen}\,K_x + 2\widetilde{M}\,\mathrm{sen}\,2K_x \\
&+ \widetilde{C}\,\mathrm{sen}\,K_x\cos K_y + \widetilde{D}\cos K_x\,\mathrm{sen}\,K_y \\
&+ \widetilde{E}\,\mathrm{sen}\,K_x\cos 2K_y + \widetilde{F}\cos K_x\,\mathrm{sen}\,2K_y \\
&+ 2\widetilde{G}\,\mathrm{sen}\,2K_x\cos K_y + 2\widetilde{H}\cos 2K_x\,\mathrm{sen}\,K_y \\
&+ 2\widetilde{J}\,\mathrm{sen}\,2K_x\cos 2K_y + 2\widetilde{K}\cos 2K_x\,\mathrm{sen}\,2K_y, \quad (13)\\
(1/2)\dot{Y} &= \widetilde{B}\,\mathrm{sen}\,K_y + 2\widetilde{N}\,\mathrm{sen}\,2K_y \\
&+ \widetilde{C}\cos K_x\,\mathrm{sen}\,K_y + \widetilde{D}\,\mathrm{sen}\,K_x\cos K_y \\
&+ 2\widetilde{E}\cos K_x\,\mathrm{sen}\,2K_y + 2\widetilde{F}\,\mathrm{sen}\,K_x\cos 2K_y \\
&+ \widetilde{G}\cos 2K_x\,\mathrm{sen}\,K_y + \widetilde{H}\,\mathrm{sen}\,2K_x\cos K_y \\
&+ 2\widetilde{J}\cos 2K_x\,\mathrm{sen}\,2K_y + 2\widetilde{K}\,\mathrm{sen}\,2K_x\cos 2K_y, \quad (14)\\
\dot{K_x} &= -V_X, \quad (15)\\
\dot{K_y} &= -V_Y; \quad (16)
\end{aligned}
$$

the list of the "tilde" symbols used in (13) and (14) is defined in the Appendix A.

We now set up about constructing the effective Hamiltonian $H^{eff} \equiv H(X, Y, K_x, K_y)$ from the system (13)-(16). The Hamilton equations in the space of the effective coordinates $Z,\ K_z$ must be satisfied:

$$\dot{Z} = H^{eff}_{K_z},\ \ \dot{K_z} = -H^{eff}_{Z}; \quad (17)$$

the expression for $\dot{Z}$ in (17) is substituted from (13), (14) and combined together with (15), (16) to give

$$
\begin{aligned}
&H^{eff} = \\
&- 2\widetilde{A}\cos K_x - 2\widetilde{B}\cos K_y - 2\widetilde{M}\cos 2K_x - 2\widetilde{N}\cos 2K_y \\
&- (\widetilde{C}+\widetilde{D})\cos(K_x+K_y) - (\widetilde{C}-\widetilde{D})\cos(K_x-K_y) \\
&- (\widetilde{E}+\widetilde{F})\cos(K_x+2K_y) - (\widetilde{E}-\widetilde{F})\cos(K_x-2K_y) \\
&- (\widetilde{G}+\widetilde{H})\cos(2K_x+K_y) - (\widetilde{G}-\widetilde{H})\cos(2K_x-K_y) \\
&- (\widetilde{J}+\widetilde{K})\cos(2K_x+2K_y) - (\widetilde{J}-\widetilde{K})\cos(2K_x-2K_y) \\
&+ V(X,Y) + \Omega, \quad (18)
\end{aligned}
$$

where Ω is a constant term independent of the dynamical coordinates $Z,\ K_z$. It is now clear that the "tilde" symbols referred to in (13) and (14) constitute the effective hopping elements characteristic of the effective tight-binding Hamiltonian H^{eff} in (18).

As a first crosscheck calculation of (18) we can test it for the case of the null electric field $\mathbf{f} = 0$ and a linear static potential $V(X, Y) = \alpha X + \beta Y$ (dropping the constant term Ω):

$$
\begin{aligned}
&H^{eff} \\
&= -2\widetilde{A}\cos K_x - 2\widetilde{B}\cos K_y \\
&- (\widetilde{C}+\widetilde{D})\cos(K_x+K_y) - (\widetilde{C}-\widetilde{D})\cos(K_x-K_y) \\
&+ \alpha X + \beta Y, \\
&= -2AF_{x0}\cos K_x - 2BF_{y0}\cos K_y \\
&- CF_{xm}F_{-ym}\cos(K_x+K_y) - CF_{xm}F_{ym}\cos(K_x-K_y) \\
&+ \alpha X + \beta Y, \\
&= -2A\cos K_x - 2B\cos K_y - 2C\cos K_x\cos K_y + \alpha X + \beta Y. \quad (19)
\end{aligned}
$$

By using Hamilton's equations $\dot{Z} = H^{eff}_{K_z}, \dot{K_z} = -H^{eff}_{Z}$ in (17) for $Z = X, Y$, we obtain

$$
\begin{aligned}
\dot{X} &= -2A\,\mathrm{sen}\,\alpha t - 2C\,\mathrm{sen}\,\alpha t\cos\beta t, \\
\dot{Y} &= -2B\,\mathrm{sen}\,\beta t - 2C\cos\alpha t\,\mathrm{sen}\,\beta t, \quad (20)
\end{aligned}
$$

which describe, as expected, a 2D Bloch oscillation with period $T = 2p\pi/\alpha$ ($p = min(n, m)$) for the rational quotient $\alpha/\beta = n/m$.

3. INTERACTIONS ENGINEERING AND RELATION TO AN LC CIRCUIT

With the explicit form of the effective Hamiltonian H^{eff} in (18) in terms of the Fourier components f_{zn} of the electric field *via* (B31), we may ask now which components will yield specific values of the effective hopping elements in H^{eff} that determine thus the transport properties of the particle in a square lattice when acted upon by the external fields. This is the "interactions engineering" scheme considered in this paper, particularly, as an extension of the one-dimensional case investigated by Mamani *et al.* (Mamani 2017). For the purpose of illustrating such interactions engineering, we choose as a case study the emulation of an LC circuit with discrete charge that has an effective Hamiltonian of the form (as we will see later in this section)

$$
\begin{aligned}
H_{LC} = &- 2\widetilde{C}\cos K_x\cos K_y - 2\widetilde{M}\cos 2K_x - 2\widetilde{N}\cos 2K_y \\
&+ V(X,Y), \quad (21)
\end{aligned}
$$

where the static potential is the quadratic form $V(X, Y) \propto X^2 + Y^2 + (X - Y)^2$ such that its second derivatives are $V_{XX} = V_{YY} = -2V_{XY}$. In this case, and for the square lattice with $A = B$, the effective hopping elements become (Appendix A):

$$\widetilde{A} = AF_{x0} - ACV_{XX}(F_{xp}F_{xm}F_{y(m+p)}/m^2)\epsilon^2,$$
$$\widetilde{B} = BF_{y0} - ACV_{XX}(F_{xp}F_{xm}F_{y(-m+p)}/m^2)\epsilon^2,$$
$$\widetilde{C} = (C/2)(F_{xm}F_{-ym} + F_{xm}F_{ym}) - A^2V_{XX}(F_{-xm}F_{ym}/m^2 - F_{xm}F_{ym}/m^2)\epsilon^2,$$
$$\widetilde{D} = (C/2)(F_{xm}F_{-ym} - F_{xm}F_{ym}) - A^2V_{XX}(F_{-xm}F_{ym}/m^2 + F_{xm}F_{ym}/m^2)\epsilon^2,$$
$$\widetilde{E} = -\widetilde{F} = ACV_{XX}(F_{xp}F_{ym}F_{y(-m+p)}/m^2)\epsilon^2,$$
$$\widetilde{G} = -\widetilde{H} = ACV_{XX}(F_{xp}F_{xm}F_{y(m+p)}/m^2)\epsilon^2,$$
$$\widetilde{J} = -\widetilde{K} = (C^2/2)V_{XX}(F_{xp}F_{xq}F_{y(m+p)}F_{y(-m+q)}/m^2)\epsilon^2,$$
$$\widetilde{M} = (A^2/2)V_{XX}(F_{xm}F_{-xm}/m^2)\epsilon^2,$$
$$\widetilde{N} = (A^2/2)V_{XX}(F_{ym}F_{-ym}/m^2)\epsilon^2; \quad (22)$$

sums are performed on the terms with the repeated indices $m,\ p,\ q$ and the variable m. Since our perturbative calculations were performed consistently up to second order in $\epsilon \equiv 1/\omega$, the effective hopping elements in (22) can be expressed as combinations of the zeroth (dominant) and 2nd order terms: $\widetilde{A} = \widetilde{A}^{(0)} + \widetilde{A}^{(2)}$, $\widetilde{B} = \widetilde{B}^{(0)} + \widetilde{B}^{(2)}$, $\widetilde{C} = \widetilde{C}^{(0)} + \widetilde{C}^{(2)}$, $\widetilde{D} = \widetilde{D}^{(0)} + \widetilde{D}^{(2)}$, $\widetilde{E} = \widetilde{E}^{(2)}$, $\widetilde{G} = \widetilde{G}^{(2)}$, $\widetilde{J} = \widetilde{J}^{(2)}$, $\widetilde{M} = \widetilde{M}^{(2)}$, $\widetilde{N} = \widetilde{N}^{(2)}$.

Now, the F_{zm} terms in (22) depend on the specific oscillating electric field $\mathbf{f} = (f_x, f_y)$ through its Fourier components. For the purpose sought in this work, we find that those components should be

$$f_x(\omega t) = 2f_{x1}\cos(\omega t) + 2f_{x2}\cos(2\omega t),$$
$$f_y(\omega t) = 2f_{y1}\cos(\omega t) + 2f_{y2}\cos(2\omega t). \quad (23)$$

Then, the expression for F_{zm} in (B31) readily becomes

$$F_{zm} = \sum_p J_{m-2p}(2f_{z1})J_p(f_{z2}); \quad (24)$$

notice the property $F_{(-z)m} = F_{z(-m)} \equiv F_{-zm}$. In order to solve the infinite sum in (24) and verify its convergence, we use the integral representation for $J_n(z)$:

$$J_n(z) = \frac{i^{-n}}{\pi}\int_0^\pi e^{iz\cos\theta}\cos(n\theta)d\theta. \quad (25)$$

Replacing this $J_n(z)$ in F_{zm} and using $\sum_p \exp[ip(C+\phi)] = \pi\delta(C+\phi)$ (for $0 < \phi < \pi$) we obtain

$$F_{zm} = \frac{i^{-m}}{\pi}\int_0^\pi e^{2if_{z1}\cos\theta}\cos[m\theta + f_{z2}\,\mathrm{sen}(2\theta)]d\theta. \quad (26)$$

Now, we set $f_{x2} = f_{y1} = 0$ in (23) as the condition to find the required form of H_{LC} ($\widetilde{D}^{(0)} = 0$ in this case) with the parameters $f_{x1},\ f_{y2}$ such that:

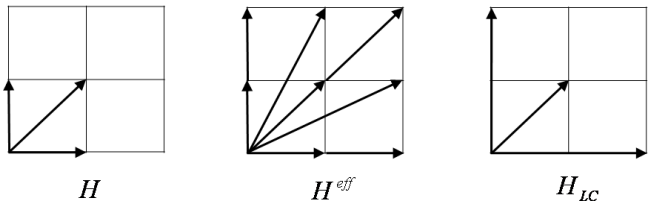

FIG. 1.— Representations of the interactions in the square lattice (from left to right): the time-dependent Hamiltonian H in (1), the effective Hamiltonian H^{eff} in (18), the Hamiltonian H_{LC} in (29) obtained by choosing specific values of the external fields (interactions engineering).

$$\widetilde{A}^{(0)} = 0 \to F_{x0} = 0 \to J_0(2f_{x1}) = 0,$$
$$\widetilde{B}^{(0)} = 0 \to F_{y0} = 0 \to \int_0^\pi \cos[f_{y2}\,\mathrm{sen}(2\theta)]\,d\theta = 0; \quad (27)$$

then, we chose from the set of solutions $\{f_{x1}, f_{y2}\}$ of (27) those which satisfy the condition that $\widetilde{A}^{(2)}$, $\widetilde{B}^{(2)}$, $\widetilde{E}$, $\widetilde{G}$, $\widetilde{J}$ should be negligible as compared to $\widetilde{M}$ and $\widetilde{N}$. One way of doing this is to calculate the euclidian norm

$$\Delta(f_{x1}, f_{y2}) \equiv \sqrt{(\widetilde{A}^{(2)})^2 + (\widetilde{B}^{(2)})^2 + (\widetilde{E})^2 + (\widetilde{G})^2 + (\widetilde{J})^2} \quad (28)$$

such that $\Delta/\widetilde{M} + \Delta/\widetilde{N}$ attains a minimum value for negative values of $\widetilde{C}$, $\widetilde{M}$, $\widetilde{N}$. Thus, with this condition and those of (27) fulfilled, the effective Hamiltonian in (18) becomes

$$H^{eff} = -2\widetilde{A}^{(2)}\cos K_x - 2\widetilde{B}^{(2)}\cos K_y - 2\widetilde{M}\cos 2K_x - 2\widetilde{N}\cos 2K_y - (\widetilde{C} + \widetilde{D}^{(2)})\cos(K_x + K_y) - (\widetilde{C} - \widetilde{D}^{(2)})\cos(K_x - K_y) - 2\widetilde{E}\cos(K_x - 2K_y) - 2\widetilde{G}\cos(2K_x - K_y) - 2\widetilde{J}\cos(2K_x - 2K_y) + V(X,Y)$$
$$\cong -2\widetilde{C}^{(0)}\cos K_x\cos K_y - 2\widetilde{M}\cos 2K_x - 2\widetilde{N}\cos 2K_y + V(X,Y), \quad (29)$$

thus attaining the required approximation $H_{LC} \cong H^{eff}$. Fig. 1 shows an schematic representation of the interactions in the square lattice (from left to right): the time-dependent Hamiltonian H in (1) is transformed into the effective Hamiltonian in H^{eff} (18) (with all the reparametrized and induced interactions) by the action of the external oscillating and static fields and, finaly, by choosing specific values of the those fields ("interactions engineering"), the Hamiltonian H_{LC} in (29) is obtained.

The numerical results found from (27) and (28) within the interval $0 < f_{x1}, f_{y2} < 100$ (with physical units restored) are

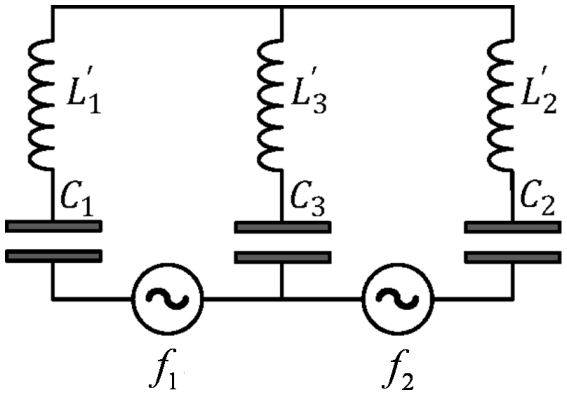

FIG. 2.— Two-mesh LC circuit.

$$
\begin{aligned}
&(q_e a/\hbar\omega)\{f_{x1}, f_{y2}\} = \{16.887, 5.519\},\\
&C^{-1}\widetilde{C}^{(0)} = -0.060,\\
&[V_{XX}A^2a^2/(\hbar\omega)^2]^{-1}\widetilde{M} = -0.021,\\
&[V_{XX}A^2a^2/(\hbar\omega)^2]^{-1}\widetilde{N} = -0.028,\\
&[V_{XX}ACa^2/(\hbar\omega)^2]^{-1}\widetilde{A}^{(2)} = 0.002,\\
&[V_{XX}ACa^2/(\hbar\omega)^2]^{-1}\widetilde{B}^{(2)} = -0.002,\\
&[V_{XX}ACa^2/(\hbar\omega)^2]^{-1}\widetilde{E} = 0.001,\\
&[V_{XX}ACa^2/(\hbar\omega)^2]^{-1}\widetilde{G} = 0.002,\\
&[V_{XX}C^2a^2/(\hbar\omega)^2]^{-1}\widetilde{J} = 0.005,\\
&\Delta/\widetilde{M} + \Delta/\widetilde{N} = 0.440. \qquad (30)
\end{aligned}
$$

We expect that $V_{XX}A^2a^2/(\hbar\omega)^2$ has an upper bound in order to have consistent results, i.e., $\widetilde{C}^{(0)}$ dominant with respect to $\widetilde{M}$ and $\widetilde{N}$. This is of course the case when $\omega \to \infty$ but, as we will see at the end of this section, ω must also have an upper bound if an analogy between the square lattice and the LC circuit is to be achieved. We think that values of the physical parameters can be found that meet reasonably such a requirement.

We now set up about describing the LC circuit depicted in Fig. 2. Following the construction of the quantum Hamiltonian operator for a two-ring system (Flores 2002), we can construct the Hamiltonian function of a two-mesh LC circuit with discrete charge q_e as

$$
\begin{aligned}
&H(q_1, q_2, \phi_1, \phi_2, q_e; t) =\\
&\quad \frac{2\hbar^2}{L_1 q_e^2}\,\mathrm{sen}^2\left(\frac{\phi_1 q_e}{2\hbar}\right) + \frac{2\hbar^2}{L_2 q_e^2}\,\mathrm{sen}^2\left(\frac{\phi_2 q_e}{2\hbar}\right)\\
&+ \frac{2\hbar^2}{L_3 q_e^2}\,\mathrm{sen}\left(\frac{\phi_1 q_e}{2\hbar}\right)\mathrm{sen}\left(\frac{\phi_2 q_e}{2\hbar}\right)\\
&+ \frac{q_1^2}{2C_1} + \frac{q_2^2}{2C_2} + \frac{(q_1 - q_2)^2}{2C_3} + q_1 f_1(\omega' t) + q_2 f_2(\omega' t), \qquad (31)
\end{aligned}
$$

which follows from the replacement of the magnetic flux as $\phi_i \to (2\hbar/q_e)\,\mathrm{sen}(q_e\phi_i/2\hbar)$ in the corresponding continuous-charge Hamiltonian function

Square lattice	**Two-mesh LC circuit**
$a = 100$ Å	$q_e \cong 1.6 \times 10^{-19}$ C
$\omega = 10^{12}$ Hz	$\omega' = 1.934 \times 10^{13}$ Hz
$f_{x1} = 1.055 \times 10^6$ V/m $f_{y2} = 0.345 \times 10^6$ V/m	$f_1 = 6.249 \times 10^{-3}$ V $f_2 = 0$
$V_{XX} = 2 \times 10^{-6}$ J/m^2	$C_1 = C_2 = C_3$ $= 2.56 \times 10^{-16}$ F
$A, C = 10^{-3}$ eV $\widetilde{C}^{(0)} = -0.060A$ $\widetilde{M} = -0.021A$ $\widetilde{N} = -0.028A$	$L_1' = L_2' \cong 0.4L_3'$ $L_3' = 9.766 \times 10^{-8}$ H

TABLA 1
NUMERICAL VALUES OF THE PHYSICAL PARAMETERS. THE VALUES OF a, ω, A, C WERE CHOSEN SO AS TO RESEMBLE TYPICAL VALUES IN A GAAS-TYPE SEMICONDUCTOR SUPERLATTICE; $f_2 = 0$ WAS SUGGESTED SO AS TO FACILITATE THE CALCULATIONS. THE OTHER VALUES RESULT FROM COMPARING THE TERMS AND ARGUMENTS OF THE EFFECTIVE HAMILTONIANS (33) AND (21), AND FROM THE CORRESPONDING ALGEBRAIC AND NUMERICAL MANIPULATIONS.

$$
\begin{aligned}
&H(q_1, q_2, \phi_1, \phi_2; t) =\\
&\frac{\phi_1^2}{2L_1} + \frac{\phi_2^2}{2L_2} + \frac{\phi_1\phi_2}{2L_3} + \frac{q_1^2}{2C_1} + \frac{q_2^2}{2C_2} + \frac{(q_1 - q_2)^2}{2C_3}\\
&+ q_1 f_1(\omega' t) + q_2 f_2(\omega' t), \qquad (32)
\end{aligned}
$$

where we have defined: $1/L_1 \equiv (L_2' + L_3')/\Upsilon$, $1/L_2 \equiv (L_1' + L_3')/\Upsilon$ and $1/L_3 \equiv 2L_3'/\Upsilon$, with $\Upsilon \equiv (1/2)\sum_{i\neq j} L_i' L_j'$; as can be readily checked the flux ϕ_i remains invariant in the limit $q_e \to 0$ yielding, as required, $H(q_1, q_2, \phi_1, \phi_2, q_e; t) \to H(q_1, q_2, \phi_1, \phi_2; t)$. In this case, the term $\phi_1\phi_2/(2L_3)$ in (32) is derived from the energy term $(1/2)L_3'(\dot{q}_1 - \dot{q}_2)^2$ according to the Kirchhoff's laws. The mutual inductance terms corresponding to this circuit are $\phi_1\phi_2/M_{12}$, $\phi_1\phi_3/M_{13}$ and $\phi_2\phi_3/M_{23}$ but we have not considered them in (32) since we did not specify the form of the couplings among L_1', L_2' and L_3'. In fact, the "mesoscopic" character of this circuit lies upon the discrete nature and small quantity (about 10) of the elementary electric charges being allocated in the capacitors and not necessarily upon the small size of the circuit which would imply couplings among the inductors.[4]

Following the standard quantum time-average techniques (Rahav 2003; Calcina-Nogales 2020) and setting the canonical transformations $\phi_1 = \Phi_1 + \pi\hbar/q_e$ and $\phi_2 = \Phi_2 + \pi\hbar/q_e$, we obtain from (32) the effective Hamiltonian function[5]

[4] Interestingly, the phenomenon of current magnification referred to by Flores and Utreras (Flores 2002) for two coupled inductances would also occur in the two-mesh circuit with three inductances studied in our work; progress is being carried on by us in that direction.

[5] The resulting Hamiltonian operator corresponds to the Hamilto-

$$H(Q_1,Q_2,\Phi_1,\Phi_2) = \frac{\hbar^2}{\overline{L}_1 q_e^2}\cos\left(\frac{\Phi_1 q_e}{\hbar}\right) + \frac{\hbar^2}{\overline{L}_2 q_e^2}\cos\left(\frac{\Phi_2 q_e}{\hbar}\right) + \frac{2\hbar^2}{\overline{L}_3 q_e^2}\cos\left(\frac{\Phi_1 q_e}{2\hbar}\right)\cos\left(\frac{\Phi_2 q_e}{2\hbar}\right) + \frac{Q_1^2}{2C_1} + \frac{Q_2^2}{2C_2} + \frac{(Q_1-Q_2)^2}{2C_3}, \quad (33)$$

where, for the case of the AC source voltages $f_1(\omega' t) = 2f_1\cos(\omega' t)$ and $f_2(\omega' t) = 2f_2\cos(2\omega' t)$, we obtain

$$\frac{1}{\overline{L}_1} \equiv \frac{1}{L_1} J_0\left(\frac{2f_1 q_e}{\hbar\omega'}\right), \quad \frac{1}{\overline{L}_2} \equiv \frac{1}{L_2} J_0\left(\frac{f_2 q_e}{\hbar\omega'}\right), \quad \frac{1}{\overline{L}_3} \equiv \frac{1}{L_3}\sum_n J_{2n}\left(\frac{f_1 q_e}{\hbar\omega'}\right) J_n\left(\frac{f_2 q_e}{2\hbar\omega'}\right). \quad (34)$$

By comparing the terms and arguments of $H(Q_1,Q_2,\Phi_1,\Phi_2)$ in (33) with those of $H_{LC}(X,Y,K_x,K_y)$ in (21) we can verify, as expected, that the required form of H_{LC} is attained for static potential energies $V(Q_1,Q_2)$ and $V(X,Y)$ whose second derivatives are related as $V_{Q_1Q_1}/V_{XX} = V_{Q_2Q_2}/V_{YY} = V_{Q_1Q_2}/V_{XY} = (a/q_e)^2$. Specifically, by choosing equal capacitances in (33), we should have that $V_{XX} = 2(q_e/a)^2/C_1$.

From the numerical values of f_{x1}, f_{y2}, $\widetilde{M}$, $\widetilde{N}$ and $\widetilde{C} \cong \widetilde{C}^{(0)}$ found in (30), we may now express the equivalence among the coefficients of $H(Q_1,Q_2,\Phi_1,\Phi_2)$ and $H_{LC}(X,Y,K_x,K_y)$ in the compact notation that comprises the three equations

$$\frac{1}{\overline{L}_1} : \frac{1}{\overline{L}_2} : \frac{2}{\overline{L}_3} = \widetilde{M} : \widetilde{N} : \widetilde{C}, \quad (35)$$

whence the the source voltage amplitudes f_1, f_2 and the inductances can be found. We may take $L_1' = L_2'$ for simplicity, thus, from $1/\overline{L}_1 : 1/\overline{L}_2 = \widetilde{M} : \widetilde{N}$ in (35), we have that $J_0(q_e f_2/\hbar\omega')/J_0(2q_e f_1/\hbar\omega') \cong 4/3$ which is satisfied for an infinte set of solutions, for example, $(q_e/\hbar\omega')f_1 = 0.517$ and $(q_e/\hbar\omega')f_2 = 0$ (although $f_2 = 0$ was so chosen just to facilitate the calculations, such a value still deserves a further phyisical interpretation). For these values, and by setting $-2\widetilde{M} = (\hbar/q_e)^2/\overline{L}_1$, $-2\widetilde{C}^{(0)} = 2(\hbar/q_e)^2/\overline{L}_3$ in the Hamiltonians (21), (33), respetively, we find

$$\frac{L_1'}{L_3'} \cong 1.4\left(\frac{q_e}{\hbar}\right)^2\frac{A^2/C}{C_1\omega^2} - 1, \quad \frac{L_1'(L_1'+2L_3')}{L_3'} \cong 25\left(\frac{\hbar}{q_e}\right)^2\frac{1}{C}. \quad (36)$$

nian function obtained with the semiclassical scheme, as was already done in the case of the single-mesh LC circuit (Mamani 2018).

As we can see, the term $(q_e/\hbar)^2(A^2/C)/(C_1\omega^2)$ has to have a lower bound to yield positive inductances; such a bound will be determined by the characteristics of the square lattice which, in this work, can be thought of as a 2D semiconductor superlattice of the GaAs type (and whose 1D version was where Bloch oscillations were first observed). Thus, we may take as typical values:

$$A, C \sim 1 \text{ meV}, \quad a \sim 100 \text{ Å}, \quad f_{x1}, f_{y2} \sim \hbar\omega/(aq_e) \sim 10^5 \text{ V/m}. \quad (37)$$

From the latter we have an estimation of $\omega \sim 10^{12}$ Hz. Since $V_{XX}(Aa/\hbar\omega)^2 = (Aq_e/\hbar)^2/(C_1\omega^2) \sim 10^{-22}$ J should hold in (30), we have then the estimation of $C_1 \sim 10^{-16}$ F. With these values, we have therefore from (36) that $L_1' \cong 0.4L_3'$ and $L_3' \sim 10^{-7}$ H. Finally, an estimation of the sources frequency ω' can be made by assuming that a maximum of just few electrons is to be alloted in a (small) mesoscopic capacitor, which is other way for interpreting the meaning of "discrete charge" LC circuit. We may take then $Q_{1,max} = 10q_e$, which, together with $C_1 = Q_{1,max}/f_1$ and $f_1 \sim \hbar\omega'/q_e$, yields $f_1 \sim 10^{-2}$ V and $\omega' \sim 10^{13}$ Hz. More precise values for the results of our numerical simulations and from comparing the terms and arguments of the effective Hamiltonians (33) and (21) are summarized in Table 1 .

We may now validate the consistency of the semiclassical model invoked in our work: the value of the frequency $\omega = 10^{12}$ Hz corresponds to an external field wavelength $\lambda \sim 10^{-3}$ m, while the lattice constant is $a = 100$ Å. The quantum wavepacket size can be taken from Mamani *et al.* (Mamani 2017), where the semiclassical method has proved to be consistent with the formal quantum approach for a wavepacket initial width $\Delta x = 10a$. We have therefore that $\lambda \gg \Delta x \gg a$, as required for the validity of the semiclassical method (see, for example Ashcroft and Mermin (1976)), and which in turn implies that the intensity of the external electric field $|\mathbf{f}| \sim 10^6$ V/m is low enough for a single-band tight-binding model Hamiltonian to hold.

By solving numerically the system of equations (17) for $X(t)$, $Y(t)$, $Q_1(t)$, $Q_2(t)$, with the values reported in Table 1, we may relate the electronic dynamics in both equivalent systems, the square lattice and the two-mesh LC circuit. Since we have managed the electric fields and the voltage sources in the former and latter systems, respectively, so as to have $H_{LC}(X,Y,K_x,K_y) \cong H_{LC}(Q_1,Q_2,\Phi_1,\Phi_2)$, then their common energies are 0.218 meV, corresponding to the initial values $X(0) = Y(0) = 0.02a$ of the effective position coordinates. We observe in Fig. 3(a(1)) a predominately diagonal oscillating motion –although not a simple one– of the particle's position about the origin of the effective position XY plane of the square lattice, which corresponds also to a predominately symmetric distribution of oscillating charges in the two-mesh LC circuit, as seen in Fig. 3(b(1)), in accordance with the diagram for H_{LC} in Fig. 1, where the diagonal hopping element is the dominant

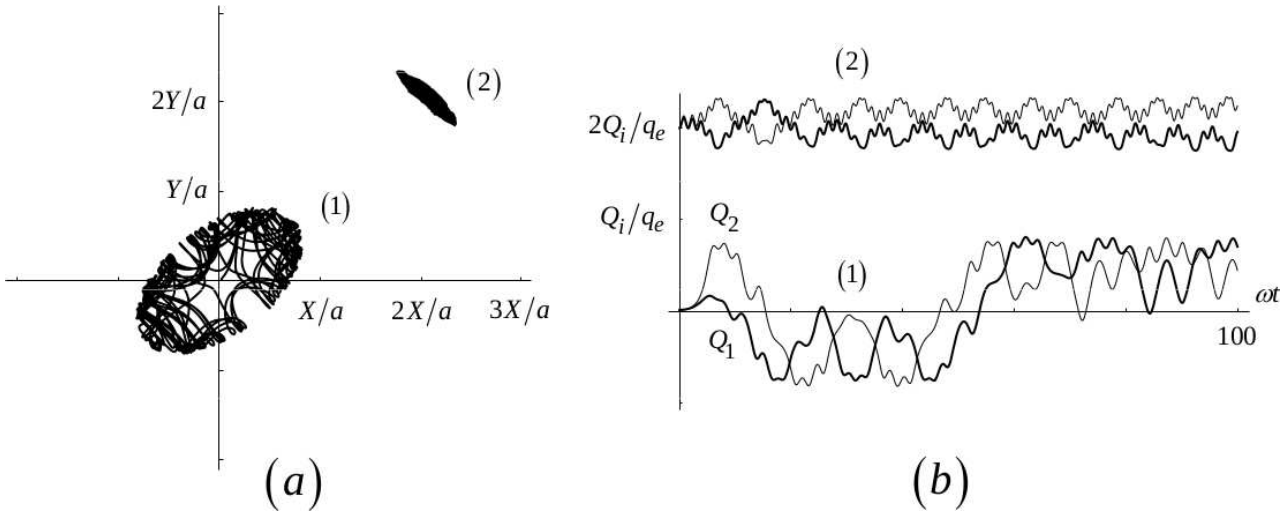

FIG. 3.— Cases of electronic motion in: (a) the effective position XY plane, and (b) the two-mesh LC circuit. In case (a) the displacements are measured in units of the lattice constant $a = 100$ Å; in case (b) the capacitors' electric charges are measured in units of the electron's charge q_e, the time is measured in units of the frequency inverse $1/\omega = 10^{-12}$ s. Cases (1) and (2) in both (a) and (b) correspond to oscillations with zero and positive time-averages, respectively. Cases (1) and (2) in (b) resemble very much the AC and DC regimes, respectively, deduced in the one-mesh LC circuit (Mamani 2018) as a consequence of a bifurcation condition.

one. Such a behavior, however, may change abruptly –as a function of the total energy, for example– giving rise to a DC regime or a supression of the mesh currents, as it does in the one-dimensional case of the one-mesh LC circuit (Mamani 2018), where we have showed that a bifurcation condition on the $\dot{Q} - Q$ phase diagram can be associated to such an abrupt change. Figs. 3(a(2)) and 3(b(2)) show position and charge oscillations with positive time-averages corresponding to an energy of 2.707 meV, contrasting with those of Figs. 3(a(1)) and 3(b(1)). The extension of the one-dimensional bifurcation condition to the two-dimensional case of the two-mesh circuit and its relation to the particle's propagation in the square lattice is an interesting issue worth to be treated elsewhere.

4. CONCLUSIONS

We have established the formal equivalence between two physical systems by means of the interactions engineering scheme developed in this paper. Those systems are: (i) a square lattice wherein an tight-binding electron propagates under the combined action of an external high-frequency and homogeneous electric field and a quadratic static potential, and (ii) a two-mesh LC circuit with discrete charge. Such formal equivalence is attained by describing both systems by effective Hamiltonian functions having the same form and whose parameters can be numerically calculated when the Hamiltonian terms are correspondingly compared among them; for deriving such effective Hamiltonians we have used perturbative expansions up to ω^{-2} when $\omega \to \infty$. Interestingly, we have found that the sought equivalence between the square lattice and the LC circuit is achieved when we choose specific values of the oscillating electric field acting upon the lattice so that the 1st neighbor interactions ($\widetilde{A}^{(0)}$, $\widetilde{B}^{(0)}$, order ω^0) are suppressed and the remaining 2nd neighbor interactions ($\widetilde{C}^{(0)}$, order ω^0) and 3rd neighbor interactions ($\widetilde{M}$, $\widetilde{N}$, order ω^{-2}) become comparable (see Table 1).

We now suggest some interesting issues that could be worth exploring further: (a) In a previous work we have investigated the relation between a single-mesh LC circuit (with discrete charge) and a charged particle hopping in a one-dimensional lattice (Mamani 2018); in the present work we have extended such an analogy to a two-mesh LC circuit and a square lattice. Thus, it seems natural to inquire whether the extension to a three-mesh LC circuit and a cubic lattice would be valid, mainly, because the one-dimensional and the square lattices do not exist as such (to our knowledge), but the three dimensional cubic lattice does exist (although not with the superlattice parameters specified in Table 1). (b) Another natural extension of our work would be considering a rectangular lattice where, for example, the sides have an incommensurate ratio of $\sqrt{3}$. In fact, this latter case would be the best suited for simulating the dynamics of a hopping electron in graphene. (c) Finally, and motivated by the results in Fig. 3(a) for the square lattice, we may suggest that the "AC regime" would indicate a quantum regime where the electronic probability densities corresponding to neighbor lattice sites overlap, which indicates in turn a higher electric conductivity, as compared to the "DC regime". Thus, a higher and a lower conducting regimes could be separated by a semiclassical bifurcation condition.

APÉNDICE

A. DEFINITIONS OF THE EFFECTIVE HOPPING ELEMENTS

The "tilde" symbols used in (13) and (14) that constitute the effective hopping elements of H^{eff} in (18) are defined as:

$$\widetilde{A} = AF_{x0} + \frac{1}{2}BC\left[\left(\Gamma_{11}^{01} - \Gamma_{11}^{11}\right)V_{XY} - \left(\Gamma_{11}^{01} + \Gamma_{11}^{11}\right)V_{YY}\right]\epsilon^2,$$

$$\widetilde{B} = BF_{y0} + \frac{1}{2}AC\left[\left(\Gamma_{10}^{10} - \Gamma_{10}^{11}\right)V_{XY} - \left(\Gamma_{10}^{10} + \Gamma_{10}^{11}\right)V_{XX}\right]\epsilon^2,$$

$$\widetilde{C} = \frac{1}{2}C(\Gamma_0 + \Gamma_1) + ABV_{XY}\left(\Gamma_{01}^{0} - \Gamma_{01}^{1}\right)\epsilon^2,$$

$$\widetilde{D} = \frac{1}{2}C(\Gamma_0 - \Gamma_1) + ABV_{XY}\left(\Gamma_{01}^{0} + \Gamma_{01}^{1}\right)\epsilon^2,$$

$$\widetilde{E} = \frac{1}{2}BC\left[\left(\Gamma_{11}^{00} - \Gamma_{11}^{10}\right)V_{XY} + \left(\Gamma_{11}^{00} + \Gamma_{11}^{10}\right)V_{YY}\right]\epsilon^2,$$

$$\widetilde{F} = \frac{1}{2}BC\left[\left(\Gamma_{11}^{00} + \Gamma_{11}^{10}\right)V_{XY} + \left(\Gamma_{11}^{00} - \Gamma_{11}^{10}\right)V_{YY}\right]\epsilon^2,$$

$$\widetilde{G} = \frac{1}{2}AC\left[\left(\Gamma_{00}^{00} + \Gamma_{00}^{10}\right)V_{XX} + \left(\Gamma_{00}^{00} - \Gamma_{00}^{10}\right)V_{XY}\right]\epsilon^2,$$

$$\widetilde{H} = \frac{1}{2}AC\left[\left(\Gamma_{00}^{00} - \Gamma_{00}^{10}\right)V_{XX} + \left(\Gamma_{00}^{00} + \Gamma_{00}^{10}\right)V_{XY}\right]\epsilon^2,$$

$$\widetilde{J} = \frac{1}{8}C^2\left[\left(\Gamma_{0}^{00} + \Gamma_{1}^{01}\right)(V_{XX} + V_{YY}) + 2\left(\Gamma_{0}^{00} - \Gamma_{1}^{01}\right)V_{XY}\right]\epsilon^2,$$

$$\widetilde{K} = \frac{1}{8}C^2\left[\left(\Gamma_{0}^{00} - \Gamma_{1}^{01}\right)(V_{XX} + V_{YY}) + 2\left(\Gamma_{0}^{00} + \Gamma_{1}^{01}\right)V_{XY}\right]\epsilon^2,$$

$$\widetilde{M} = \frac{1}{4}\left[\left(2A^2\Gamma_{00}^{0} + C^2\Gamma_{0}^{01}\right)V_{XX} - C^2\Gamma_{0}^{01}V_{YY}\right]\epsilon^2,$$

$$\widetilde{N} = \frac{1}{4}\left[\left(2B^2\Gamma_{11}^{0} + C^2\Gamma_{0}^{10}\right)V_{YY} - C^2\Gamma_{0}^{10}V_{XX}\right]\epsilon^2.$$

The definitions of the "Γ" symbols used above are:

$$\begin{array}{l|l}
\Gamma_0 = F_{xm}F_{-ym} & \\
\Gamma_1 = F_{xm}F_{ym} & \\
\Gamma_{00}^{0} = F_{xm}F_{-xm}/m^2 & \Gamma_{00}^{00} = F_{xp}F_{-xm}F_{y(m-p)}/m^2 \\
\Gamma_{00}^{1} = F_{xm}F_{xm}/m^2 & \Gamma_{00}^{01} = F_{xp}F_{xm}F_{y(m-p)}/m^2 \\
\Gamma_{01}^{0} = F_{ym}F_{-xm}/m^2 & \Gamma_{00}^{10} = F_{xp}F_{xm}F_{y(m+p)}/m^2 \\
\Gamma_{01}^{1} = F_{ym}F_{xm}/m^2 & \Gamma_{00}^{11} = F_{xp}F_{-xm}F_{y(m+p)}/m^2 \\
\Gamma_{10}^{0} = F_{xm}F_{-ym}/m^2 & \Gamma_{01}^{00} = F_{xp}F_{-ym}F_{y(m-p)}/m^2 \\
\Gamma_{10}^{1} = F_{xm}F_{ym}/m^2 & \Gamma_{01}^{01} = F_{xp}F_{ym}F_{y(m-p)}/m^2 \\
\Gamma_{11}^{0} = F_{ym}F_{-ym}/m^2 & \Gamma_{01}^{10} = F_{xp}F_{ym}F_{y(m+p)}/m^2 \\
\Gamma_{11}^{1} = F_{ym}F_{ym}/m^2 & \Gamma_{01}^{11} = F_{xp}F_{-ym}F_{y(m+p)}/m^2 \\
\Gamma_{0}^{00} = F_{xp}F_{xq}F_{y(m-p)}F_{-y(m+q)}/m^2 & \Gamma_{10}^{00} = F_{xp}F_{xm}F_{-y(m+p)}/m^2 \\
\Gamma_{0}^{01} = F_{xp}F_{xq}F_{y(m-p)}F_{y(m+q)}/m^2 & \Gamma_{10}^{01} = F_{xp}F_{xm}F_{y(m+p)}/m^2 \\
\Gamma_{0}^{10} = F_{xp}F_{xq}F_{y(m-p)}F_{y(-m+q)}/m^2 & \Gamma_{10}^{10} = F_{xp}F_{xm}F_{y(-m+p)}/m^2 \\
\Gamma_{0}^{11} = F_{xp}F_{xq}F_{y(m-p)}F_{y(m-q)}/m^2 & \Gamma_{10}^{11} = F_{xp}F_{xm}F_{y(m-p)}/m^2 \\
\Gamma_{1}^{00} = F_{xp}F_{xq}F_{y(m+p)}F_{y(m-q)}/m^2 & \Gamma_{11}^{00} = F_{xp}F_{ym}F_{-y(m+p)}/m^2 \\
\Gamma_{1}^{01} = F_{xp}F_{xq}F_{y(m+p)}F_{y(-m+q)}/m^2 & \Gamma_{11}^{01} = F_{xp}F_{ym}F_{y(m+p)}/m^2 \\
\Gamma_{1}^{10} = F_{xp}F_{xq}F_{y(m+p)}F_{y(m+q)}/m^2 & \Gamma_{11}^{10} = F_{xp}F_{ym}F_{y(-m+p)}/m^2 \\
\Gamma_{1}^{11} = F_{xp}F_{xq}F_{y(m+p)}F_{-y(m+q)}/m^2 & \Gamma_{11}^{11} = F_{xp}F_{ym}F_{y(m-p)}/m^2
\end{array}$$

Sums are performed on the terms with the repeated indices $m,\ p,\ q$ and the variable m.

B. TIME-AVERAGE DERIVATION OF THE EFFECTIVE DYNAMICAL COORDINATES

In this Appendix we apply the time-average techniques that yield the system for the effective dynamical

coordinates (13)-(16). This is done by replacing the time-derivatives of the terms in (10) into the system (6)-(9) yielding:

$$\dot{X} + \omega \frac{d\xi_x}{d\tau} = 2A \operatorname{sen} \alpha_x + 2C \operatorname{sen} \alpha_x \cos \alpha_y, \tag{B1}$$

$$\dot{Y} + \omega \frac{d\xi_y}{d\tau} = 2B \operatorname{sen} \alpha_y + 2C \cos \alpha_x \operatorname{sen} \alpha_y, \tag{B2}$$

$$\dot{K_x} + \omega \frac{d\eta_x}{d\tau} = -V_x(\gamma_x, \gamma_y), \tag{B3}$$

$$\dot{K_y} + \omega \frac{d\eta_y}{d\tau} = -V_y(\gamma_x, \gamma_y), \tag{B4}$$

where we have defined $\alpha_z \equiv K_z + \eta_z - g_z$, $\gamma_z \equiv Z + \xi_z$. We will use later $\alpha_z^0 \equiv K_z + \eta_{z0} - g_z$ which results from evaluating α_z for $\epsilon = 0$, and $\alpha_z^{00} \equiv K_z - g_z$ which results from evaluating α_z^0 for $\eta_{z0} = 0$. The application of the time-average properties to the system (B1)-(B4) yields:

$$\dot{X} = 2A \langle \operatorname{sen} \alpha_x \rangle + 2C \langle \operatorname{sen} \alpha_x \cos \alpha_y \rangle, \tag{B5}$$

$$\dot{Y} = 2B \langle \operatorname{sen} \alpha_y \rangle + 2C \langle \cos \alpha_x \operatorname{sen} \alpha_y \rangle, \tag{B6}$$

$$\dot{K_x} = -\langle V_x(\gamma_x, \gamma_y) \rangle, \tag{B7}$$

$$\dot{K_y} = -\langle V_y(\gamma_x, \gamma_y) \rangle. \tag{B8}$$

Combining (B5)-(B8) and (B1)-(B4) one obtains a system for the fast coordinates:

$$\omega \frac{d\xi_x}{d\tau} = 2A \left(\operatorname{sen} \alpha_x - \langle \operatorname{sen} \alpha_x \rangle \right) + 2C \left(\operatorname{sen} \alpha_x \cos \alpha_y - \langle \operatorname{sen} \alpha_x \cos \alpha_y \rangle \right), \tag{B9}$$

$$\omega \frac{d\xi_y}{d\tau} = 2B \left(\operatorname{sen} \alpha_y - \langle \operatorname{sen} \alpha_y \rangle \right) + 2C \left(\cos \alpha_x \operatorname{sen} \alpha_y - \langle \cos \alpha_x \operatorname{sen} \alpha_y \rangle \right), \tag{B10}$$

$$\omega \frac{d\eta_x}{d\tau} = -V_x(\gamma_x, \gamma_y) + \langle V_x(\gamma_x, \gamma_y) \rangle, \tag{B11}$$

$$\omega \frac{d\eta_y}{d\tau} = -V_y(\gamma_x, \gamma_y) + \langle V_y(\gamma_x, \gamma_y) \rangle. \tag{B12}$$

The solutions of (B9)-(B12) are to be substituted in (B5)-(B8) in order to have a system of differential equations for the slow coordinates $Z,\ K_z$. To achieve that, and since the frequency ω is large, we expand the fast coordinates $\xi_z,\ \eta_z$ as power series of the small parameter $\epsilon \equiv t/\tau = 1/\omega$ up to the order of ϵ^2 with coeficients $\xi_{zi},\ \eta_{zi}$. The substitution of these series in two of the trigonometric functions and in the derivatives V_x, V_y in (B5)-(B8) leads to

$$\operatorname{sen} \alpha_x = \operatorname{sen} \alpha_x^0 + \epsilon \eta_{x1} \cos \alpha_x^0 + \left(\eta_{x2} \cos \alpha_x^0 - (1/2) \eta_{x1}^2 \operatorname{sen} \alpha_x^0 \right) \epsilon^2, \tag{B13}$$

$$\operatorname{sen} \alpha_y = \operatorname{sen} \alpha_y^0 + \epsilon \eta_{y1} \cos \alpha_y^0 + \left(\eta_{y2} \cos \alpha_y^0 - (1/2) \eta_{y1}^2 \operatorname{sen} \alpha_y^0 \right) \epsilon^2, \tag{B14}$$

$$V_x(\gamma_x, \gamma_y) = V_X^0 + \left(\xi_{x1} V_{XX}^0 + \xi_{y1} V_{XY}^0 \right) \epsilon + \left(\xi_{x2} V_{XX}^0 + \xi_{y2} V_{XY}^0 \right) \epsilon^2, \tag{B15}$$

$$V_y(\gamma_x, \gamma_y) = V_Y^0 + \left(\xi_{x1} V_{XY}^0 + \xi_{y1} V_{YY}^0 \right) \epsilon + \left(\xi_{x2} V_{XY}^0 + \xi_{y2} V_{YY}^0 \right) \epsilon^2, \tag{B16}$$

where $\gamma_{z0} \equiv Z + \xi_{z0}$; the superscript "0" in the derivatives of the potential energy means that its argument is γ_{z0} and the abscence of a superscript means that the argument is Z. Substituting (B13)-(B16) in (B9)-(B12), and comparing the terms in the same powers of ϵ, one obtains:

(i) For ϵ^0,

$$\frac{d\xi_{x0}}{d\tau} = \frac{d\eta_{x0}}{d\tau} = \frac{d\xi_{y0}}{d\tau} = \frac{d\eta_{y0}}{d\tau} = 0. \tag{B17}$$

(ii) For ϵ^1,

$$\frac{d\xi_{x1}}{d\tau} = 2A\left(\operatorname{sen}\alpha_x^{00} - \left\langle \operatorname{sen}\alpha_x^{00}\right\rangle\right) + 2C\left(\operatorname{sen}\alpha_x^{00}\cos\alpha_y^{00} - \left\langle \operatorname{sen}\alpha_x^{00}\cos\alpha_y^{00}\right\rangle\right), \tag{B18}$$

$$\frac{d\xi_{y1}}{d\tau} = 2B\left(\operatorname{sen}\alpha_y^{00} - \left\langle \operatorname{sen}\alpha_y^{00}\right\rangle\right) + 2C\left(\cos\alpha_x^{00}\operatorname{sen}\alpha_y^{00} - \left\langle \cos\alpha_x^{00}\operatorname{sen}\alpha_y^{00}\right\rangle\right), \tag{B19}$$

$$\frac{d\eta_{y1}}{d\tau} = \frac{d\eta_{x1}}{d\tau} = 0. \tag{B20}$$

(iii) For ϵ^2,

$$\frac{d\eta_{x2}}{d\tau} = -\xi_{x1}V_{XX} - \xi_{y1}V_{XY}, \tag{B21}$$

$$\frac{d\eta_{y2}}{d\tau} = -\xi_{x1}V_{XY} - \xi_{y1}V_{YY}; \tag{B22}$$

$$\frac{d\xi_{y2}}{d\tau} = \frac{d\xi_{x2}}{d\tau} = 0. \tag{B23}$$

The convenient solutions for (B17), (B20) and (B23) are chosen as $\xi_{x0} = \eta_{x0} = \xi_{y0} = \eta_{y0} = 0$, $\eta_{z1} = 0$ and $\xi_{z2} = 0$, respectively. The resulting right-hand side of the system (B5)-(B8) stands now as:

$$\dot{X} = 2A\left\langle \operatorname{sen}\alpha_x^{00}\right\rangle + 2C\left\langle \operatorname{sen}\alpha_x^{00}\cos\alpha_y^{00}\right\rangle + 2\left(A\left\langle \eta_{x2}\cos\alpha_x^{00}\right\rangle + C\left\langle \eta_{x2}\cos\alpha_x^{00}\cos\alpha_y^{00}\right\rangle - C\left\langle \eta_{y2}\operatorname{sen}\alpha_x^{00}\operatorname{sen}\alpha_y^{00}\right\rangle\right)\epsilon^2, \tag{B24}$$

$$\dot{Y} = 2B\left\langle \operatorname{sen}\alpha_y^{00}\right\rangle + 2C\left\langle \cos\alpha_x^{00}\operatorname{sen}\alpha_y^{00}\right\rangle + 2\left(B\left\langle \eta_{y2}\cos\alpha_y^{00}\right\rangle + C\left\langle \eta_{y2}\cos\alpha_x^{00}\cos\alpha_y^{00}\right\rangle - C\left\langle \eta_{x2}\operatorname{sen}\alpha_x^{00}\operatorname{sen}\alpha_y^{00}\right\rangle\right)\epsilon^2, \tag{B25}$$

$$\dot{K}_x = -V_X, \tag{B26}$$

$$\dot{K}_y = -V_Y, \tag{B27}$$

where α_z^{00} depends on K_z and on the external fields, while η_{z2} is to be found by solving (B18), (B19), (B21) and (B22). The result will be the sought system of differential equations for the slow coordinates $Z,\ K_z$ whose solution will permit us to deduce the effective Hamiltonian function $H(X, Y, K_x, K_y)$.

Let us express the trigonometric functions in (B24), (B25) in complex form:

$$\operatorname{sen}\alpha_z^{00} = \frac{1}{2i}\sum_n \left[e^{iK_z}F_{zn} - e^{-iK_z}F_{-zn}\right]e^{-in\tau}, \tag{B28}$$

$$\cos\alpha_z^{00} = \frac{1}{2}\sum_n \left[e^{iK_z}F_{zn} + e^{-iK_z}F_{-zn}\right]e^{-in\tau}, \tag{B29}$$

where we have used the following Fourier expansion given that $g_z(\tau)$ is a periodic real and odd function of t, corresponding to the real and even function $f_z(\tau)$:

$$e^{ig_z} = \sum_n F_{zn}e^{in\tau}. \tag{B30}$$

For the external field $f_z(\omega t) = 2\sum_{n=1}^{\infty} f_{zn}\cos(n\omega t)$ the coefficients F_{zn} are

$$F_{zm} = \sum_{n_1,n_2,n_3,\ldots} J_{n_1}(2f_{z1})J_{n_2}(2f_{z2}/2)J_{n_3}(2f_{z3}/3)\ldots\delta_{m,n_1+2n_2+3n_3+\ldots}\,. \tag{B31}$$

Substituting now (B28), (B29) in (B18), (B19), and solving these along with (B21), (B22) for η_{z2} we find:

$$\eta_{z2} = \frac{\partial\Lambda}{\partial Z}, \tag{B32}$$

where

$$\Lambda(X,Y) \equiv \frac{1}{2i}\sum_{n\neq 0}\Big\{2AV_X\left(e^{iK_x}F_{xn}-e^{-iK_x}F_{-xn}\right)+2BV_Y\left(e^{iK_y}F_{yn}-e^{-iK_y}F_{-yn}\right)$$
$$+C\left(V_X+V_Y\right)\left(e^{i(K_x+K_y)}F_{xm}F_{y(n-m)}-e^{-i(K_x+K_y)}F_{xm}F_{-y(n+m)}\right)$$
$$+C\left(V_X-V_Y\right)\left(e^{i(K_x-K_y)}F_{xm}F_{y(-n+m)}-e^{-i(K_x-K_y)}F_{xm}F_{y(n+m)}\right)\Big\}\frac{e^{-in\tau}}{n^2}; \qquad \text{(B33)}$$

a sum in Λ is performed on the terms with the repeated index m. Substituting now (B32), (B28) and (B29) in (B24) and (B25), and performing the time-average operations with $\left\langle e^{i(n\pm m)\tau}\right\rangle = \delta_{n,\mp m}$, we obtain the system for the effective dynamical coordinates $X,\ Y,\ K_x,\ K_y$ given in (13)-(16).

REFERENCIAS

Ashcroft N. & Mermin N. D. 1976, *Solid State Physics* (Saunders College, Philadelphia).
Bandyopadhyay M. & Dattagupta S. 2008, *Pramana J. Phys.* **70**, 381.
Calcina-Nogales M. 2003, *Mod. Phys. Lett. B* **27**, 1350138.
Calcina-Nogales M., Mamani E. & Sanjinés D. 2020, *preprint*.
Chen B. & Li Y. Q 1996, *Phys. Rev. B* **53**, 4027.
Chen B. 2005, *Phys. Lett. A* **335**, 103.
Dignam M. M. & de Sterke C. M. 2002, *Phys. Rev. Lett.* **88**, 4, 046806.
Dunlap D. H. & Kenkre V. M. 1986, *Phys. Rev. B* **34**, 3625-3633.
Flores J. C. & Utreras-Díaz C. A. 2002, *Phys. Rev. B* **66**, 153410.
Flores J. C. & Lazo E. 2005, *IEEE* **4**, 688.
Houston W. V. 1940, *Phys. Rev.* **57**, 184.
Itin A. P. & Neishtadt A. 2014, *Phys. Lett. A* **378**, 822.
Itin A. P. & Katsnelson M. I. 2015, *Phys. Rev. Lett.* **115**, 075301.
Kadirko V., Ziegler K. & Kogan E. 2013, *Graphene* **2**, 97.
Kapitza P. L. 1965, in *Collected Papers of P. L. Kapitza*, edited by ter Haar D. (Pergamon Press, Oxford); Kapitza P. L. 1951, *Zh. Eksp. Teor. Fiz.* **21**, 588.
Kittel C. 1987, *Quantum Theory of Solids* (John Wiley and Sons, New York).
Krieger J. B. & Iafrate G. J. 1986, *Phys. Rev. B* **33**, 5494.
Kundu R. 2011, *Mod. Phys. Lett. B* **25**, 163.
Landau L. D. & Lifschitz E. M. 1985, *Mecánica* (Reverté, Barcelona).
Longhi S., Dreisow F., Heinrich M., Pertsch T., Tünnermann A., Nolte S. & Szameit A. 2010, *Phys. Rev. A* **82**, 053813.
Lyssenko V., Valusis G. & Löser F. 1997, *Phys. Rev. Lett.* **79**, 301.
Madison K. W., Fischer M. C., Diener R. B., Niu Q. & Raizen M. G. 1998, *Phys. Rev. Lett.* **81**, 23, 5093.
Mamani E., Calcina-Nogales M. & Sanjinés D. 2017, *Int. J. Mod. Phys. B* **31**, 1750116.
Mamani E., Calcina-Nogales M. & Sanjinés D. 2018, *Rev. Mex. Fis.* **64**, 456-463.
Rahav S., Gilary I. & Fishman S. 2003, *Phys. Rev. A* **68**, 013820.
Reich S., Maultzsch J., Thomsen C. & Ordejón P. 2002, *Phys. Rev. B* **66**, 035412.
Rossi F. 1997, *Bloch oscillations and Wannier-Stark localization in semiconductor superlattices* (Theory of transport properties of semiconductor nanostructures, ed. E. Schoell, Chapman and Hall, London).
Wright A. R., Liu F. & Zhang C. 2009, *Nanotechnology* **20**, No. 40.